© 2007 Schattauer GmbH

3D kinematics of the interphalangeal joints in the forelimb of walking and trotting horses

H. M. Clayton, D. H. Sha, J. A. Stick, P. Robinson
Mary Anne McPhail Equine Performance Center, Department of Large Animal Clinical Sciences, College of Veterinary Medicine, Michigan State University, East Lansing, Michigan, USA

Summary
The objective was to measure 3D rotations of the distal (DIP) and proximal (PIP) interphalangeal joints at walk and trot. 3D trajectories of markers fixed to the proximal phalanx, middle phalanx and the hoof wall of the right forelimb of four sound horses were recorded at 120 Hz. Joint kinematics were calculated in terms of anatomically-based joint coordinate systems between the bone segments. Ranges of motion were similar at walk and trot. Values for the DIP joint were: flexion/extension: 46 ± 3° at walk, 47 ± 4° at trot; internal/external rotation: 5 ± 1° at walk, 6 ± 3° at trot; and adduction/abduction: 5 ± 2° at walk, 5 ± 3° at trot. Within each gait, kinematic profiles at the DIP joint were similar between horses with the exception of adduction/abduction during breakover, which may vary depending on the direction of hoof rotation over the toe. Knowledge of the types and amounts of motion at the DIP joint will be useful in understanding the aetiology and treatment of injuries to the soft tissues, which are being recognized more frequently through the use of sensitive imaging techniques. Ranges of motion for the PIP joint were: flexion/extension: 13 ± 4° at walk, 14 ± 4° at trot; adduction/abduction: 3 ± 1° at walk, 3 ± 1° at trot; and internal/external rotation: 3 ± 1° at walk, 4 ± 1° at trot. The PIP joint made a significant contribution to flexion/extension of the digit. During surgical arthrodesis, the angle of fusion may be important since loss of PIP joint extension in late stance is likely to be accommodated by increased extension of the DIP joint.

Keywords
Kinematics, joint angles, coffin joint, pastern joint, horse

Vet Comp Orthop Traumatol 2007; 20: 1–7

Introduction

Kinematic studies of equine locomotion have focused on two-dimensional (2D) analysis in the sagittal plane, which describes flexion and extension of the joints with respect to the global (laboratory) coordinate system (1-3). This type of analysis ignores abduction-adduction and axial rotations of the joints; it is important to investigate the role of these extra-sagittal motions in joint loading and in the subsequent development of lameness. Three-dimensional (3D) analysis describes flexion/extension, adduction/abduction and axial (internal/external) rotations of the joints in a coordinate system that is based on the axes of the bones and is independent of the horse's plane of motion. In the equine forelimb, *in vivo* 3D kinematics have been reported for the carpal joint at trot (4) and for the digital joints during the stance phase in four horses at walk (5) and three horses at trot (6).

The majority of equine kinematic studies have been based on tracking markers attached to the skin (3, 7-9). Skin markers provide a simple and non-invasive method of visualizing joint motion, but large errors may arise due to soft tissue movement over the underlying bone (10). Correction models have been developed to reduce these errors in 2D studies (11) and for a limited number of bone segments in 3D studies (12, 13) but algorithms to correct for skin displacement distal to the metacarpus are not available. Therefore, the proximal (P1) and middle (P2) phalanges have usually been modeled as a single, rigid segment, and any motion at the proximal interphalangeal (PIP) joint has been incorporated into the kinematics of the metacarpophalangeal (MCP) and distal interphalangeal (DIP) joints (3, 7-9). Comparisons of data from studies using skin-fixed markers versus bone-fixed markers suggests that skin displacement is significant in this region (6). To overcome the problem of artifacts due to skin displacement, bone-fixed markers have been used to measure joint kinematics accurately in man (10, 14) and horses (4, 11, 15, 16).

A few studies have used bone-fixed markers to track movements of the individual phalanges and measure kinematics of the interdigital joints (5, 6, 16). The results have shown that small amounts of adduction/abduction and axial rotation occur even when the horse moves in a straight line. Application of a 6° bilateral heel wedge affected sagittal plane kinematics with an increase in maximal flexion and a decrease in maximal extension of the PIP and DIP joints whereas a toe wedge had opposite effects (6). Extra-sagittal motions were not affected by changes in craniocaudal balance when trotting (6) though at walk heel wedges were associated with a small but significant decrease in internal rotation during hoof landing (16). In an *in vitro* study, when a 12° heel wedge was applied unilaterally, the DIP joint showed an average of 5.6° adduction/abduction with narrowing of the joint space on the side of the wedge, together with about 4.7° axial rotation away from the raised side (17). Thus, significant amounts of extra-sagittal motions of the digital joints are possible and may be used to compensate for mediolateral imbalance of the hoof (19).

Knowledge of the 3D kinematics of the digital joints may aid in understanding the mechanisms underlying digital soft tissue injuries that are being diagnosed more frequently through the use of sophisticated imaging techniques (20) and in developing appropriate rehabilitation programs for these injuries. Furthermore, descriptions of 3D kinematics are an essential step toward 3D

Received March 3, 2006
Accepted November 1, 2006

inverse dynamic analysis, which calculates mechanical variables that cannot be measured directly, such as the torques around the joints and the work done across the joints (7, 19-21). Inverse dynamic analysis offers further insight into the mechanisms by which injuries occur.

The objective of this study was to use markers fixed rigidly to P1, P2 and the hoof wall to characterize 3D rotations of the equine PIP and DIP joints in an anatomically relevant, bone-based coordinate system (BCS) during stance and swing phases for horses walking and trotting in a straight line on a firm surface.

Methods

Subjects

Four sound horses (mass: 521±20kg; height: 1.60±0.05m) were used in this study with approval of the Institutional Committee on Animal Use and Care. The horses were not shod.

Bone-fixed markers

A detailed explanation of the procedure used to fix the markers to the bones has been provided previously (15). In summary, 4.75 mm diameter Steinmann pins were inserted percutaneously under general anaesthesia into the lateral aspect of P1 and P2 of the right forelimb of each subject, to which markers were subsequently attached as described below (Fig. 1).

Post-operative care

Analgesics were administered post-surgically: 2 g phenylbutazone (Schering-Plough, Kenilworth, NJ, USA) was injected intravenously before recovery from anaesthesia, then phenylbutazone paste (Schering-Plough, Kenilworth, NJ, USA) was administered orally at a dosage of 2 g b.i.d. for two days followed by 1 g b.i.d. for a further 2 days. Just prior to data collection, 2% mepivacaine hydrochloride solution (Carbocaine-V, Pharmacia and Upjohn Company, Kalamazoo, MI) was infiltrated locally around the site of pin insertion. All subjects moved willingly and apparently normally during data collection, which took place the day following surgery. When data collection was complete, the pins were removed under local anaesthesia.

Bone coordinate systems

A triad of 15 mm diameter, reflective, spherical markers was rigidly attached to each pin during data collection (Fig. 1). A bone-based local coordinate system (BCS) was defined for each bone segment. Decisions regarding the establishment of the BCS have important effects on the results of the analysis and must, therefore, be stated clearly (22). In this study, the BCS was defined with the subject in a normal standing position. Palpation and fluoroscopy were used to identify the proximal tubercles on the medial and lateral sides and the distal tubercle on the lateral side of P1 and P2 (Fig. 1). Temporary markers, 15 mm in diameter, were placed on the skin overlying these sites during recording of stationary (stance) files. The temporary markers were used to define the BCS and to relate the bone-fixed markers to the osseous landmarks. The skin markers were removed before collecting data at walk and trot. For the hoof segment, it was assumed that movements of P3 relative to the hoof capsule were negligible, and movements of P3 were represented by three, 15 mm diameter, spherical markers fixed rigidly to the toe, the medial quarter and the lateral quarter of the hoof wall.

Right-handed coordinate systems were developed for P1 and P2 by first defining the flexion/extension axis as running from the proximolateral marker to the proximomedial marker. The adduction/abduction axis pointed dorsally, perpendicular to the plane formed by the flexion/extension axis and the axis running from the proximolateral marker to the distolateral marker. Finally, the axial (internal/external) rotation axis was defined as pointing proximally along the long axis of the bone and perpendicular to the plane formed by the flexion/extension and adduction/abduction axes. The origins of the BCS for P1 and P2 were located within the bones midway between the two proximal markers.

The BCS for P3 was defined by adding a temporary marker to the dorsal hoof wall at the toe during recording of the standing file (Fig. 1). The flexion/extension axis was defined first as running from the marker on the lateral quarter to the marker on the medial quarter. The internal/external rotation axis was defined being parallel to the axis running from the lower toe marker to the upper toe marker and directed proximally. The adduction/abduction axis pointed dorsally and was perpendicular to the plane formed by the flexion/extension axis and the internal/external rotation axis. The origin of the BCS for the distal phalanx was embedded in the

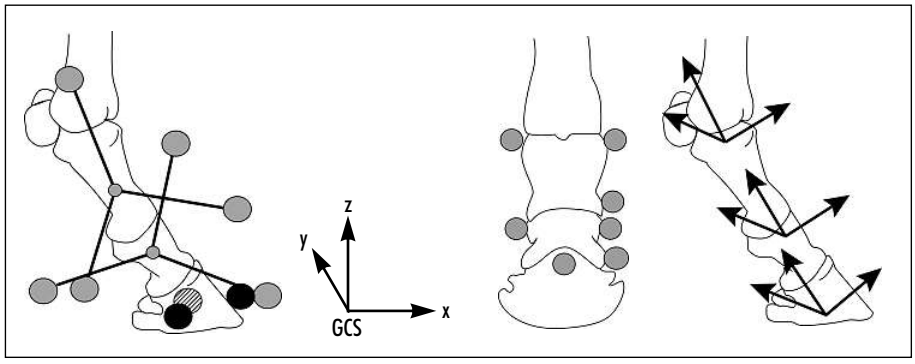

Fig. 1 Configuration of markers used in kinematic calculations. Left: Lateral view of bone-fixed marker triads and hoof-fixed markers (dark grey circles) used to track the movements of the proximal, middle and distal phalanges. Centre: Dorsal view of temporary markers attached to skin over proximal and middle phalanges and to the dorsal hoof wall (light grey circles) to establish the bone-based local coordinate systems. Right: Location and orientation of bone-based local coordinate systems for the proximal, middle and distal phalanges: x) craniocaudal axis; y) mediolateral axis; z) proximodistal axis.

Table 1 Stride characteristics for the walk and trot in the individual horses and for the group. Values are mean ± SD.

Subject	Speed (m/s)		Stride Duration (ms)		Stance Duration (% stride)		Start Breakover (% stride)	
	Walk	Trot	Walk	Trot	Walk	Trot	Walk	Trot
1	1.44±0.09	2.73±0.14	1348±44	802±24	1.44±0.09	2.73±0.14	53.8±0.8	36.8±1.6
2	1.60±0.07	2.95±0.09	1187±17	738±11	1.60±0.07	2.95±0.09	53.8±0.4	39±2.1
3	1.50±0.05	3.09±0.13	1218±26	768±21	1.50±0.05	3.09±0.13	56.2±0.8	36.4±0.6
4	1.51±0.06	3.58±0.10	1290±48	744±14	1.51±0.06	3.58±0.10	54.7±0.5	35.7±0.5
Mean ± SD	1.51±0.07	3.09±0.36	1260±72	763±29	1.51±0.07	3.09±0.36	54.6±0.8	37±1.0

bone midway between the markers at the lateral and medial quarters. It must be pointed out that the internal/external rotation axis and the flexion/extension axis may not be orthogonal if the hoof wall was asymmetrical on the medial and lateral sides.

Data collection and preprocessing

Kinematic data were recorded in the laboratory global coordinate system (GCS) using a motion analysis system with eight infrared cameras recording at 120 Hz and Realtime 4.2 software (Motion Analysis Corporation, Santa Rosa, CA, USA). A volume measuring 5 m long by 2 m wide by 3 m high was calibrated using a wand technique. The mean error in measuring a known length within the volume was 0.88 mm. The markers were tracked as each horse walked and trotted in hand at its own comfortable speed along a 40 m rubberized runway. A successful trial consisted of a single stride of the right forelimb, starting with stance. Data collected from a force platform (LG-6–4–8000, AMTI, Watertown, MA, USA) embedded in the runway were used to detect the onset and termination of right forelimb stance. Data were analyzed using custom written code in Matlab (MathWorks Inc, Natick, MA, USA). Kinematic data were filtered using a fourth-order Butterworth filter with a cutoff frequency of 12 Hz. The length of data was normalized as 101 points for a full stride. Four trials that were within a narrow range of velocities were analyzed for each horse at each gait.

Calculation of joint kinematics

To calculate joint kinematics in the sense of anatomic position (23), the locations of the marker triads in the GCS in the standing file were transformed to the corresponding BCS defined above. The orientation matrices and displacement vectors for the marker triads were then calculated for each frame recorded at stance, walk and trot using a singular value decomposition method (24). Lastly, the relative angular motions (helical angle changes) between the segments were calculated using a spatial attitude method (25, 26).

All variables were expressed relative to the value at initial ground contact of the hoof to reduce variability due to differences in conformation or orientation of the bone axes between subjects. Movements were described in terms of motion of the distal segment relative to a fixed proximal segment.

Data analysis

The range of motion in each direction was determined for each horse and for the group (mean ± SD) during stance, swing and for the entire stride. The number of subjects, which was limited to four due to the invasiveness of the procedure, did not give sufficient power to make statistical comparisons between gaits.

Results

Velocity and temporal kinematics of the walk and trot for the individual horses and for the entire group are compared in Table 1. The ranges of angular motion of the PIP and DIP joints during the stance phase, the swing phase and the entire stride (Table 2) were similar for walk and trot at both joints, with flexion/extension being the dominant rotation.

Table 2 Ranges of rotational motion at the proximal interphalangeal (PIP) and distal interphalangeal (DIP) joints of the forelimb during walking and trotting (n=4). Values are mean ± SD.

Joint	Rotation	Range of Motion					
		Stride		Stance		Swing	
		Walk	Trot	Walk	Trot	Walk	Trot
PIP	Flexion/extension (°)	13±4	14±4	10±2	10±1	10±3	11±5
DIP	Flexion/extension (°)	46±3	47±4	46±3	47±4	31±4	29±6
PIP	Int/ext rotation (°)	3±1	4±1	2±1	3±1	2±1	3±2
DIP	Int/ext rotation (°)	5±1	6±3	4±2	5±4	4±1	3±2
PIP	Adduction/abduction (°)	3±1	3±1	2±1	2±1	3±1	3±1
DIP	Adduction/abduction (°)	5±2	5±3	4±2	5±3	4±1	3±1

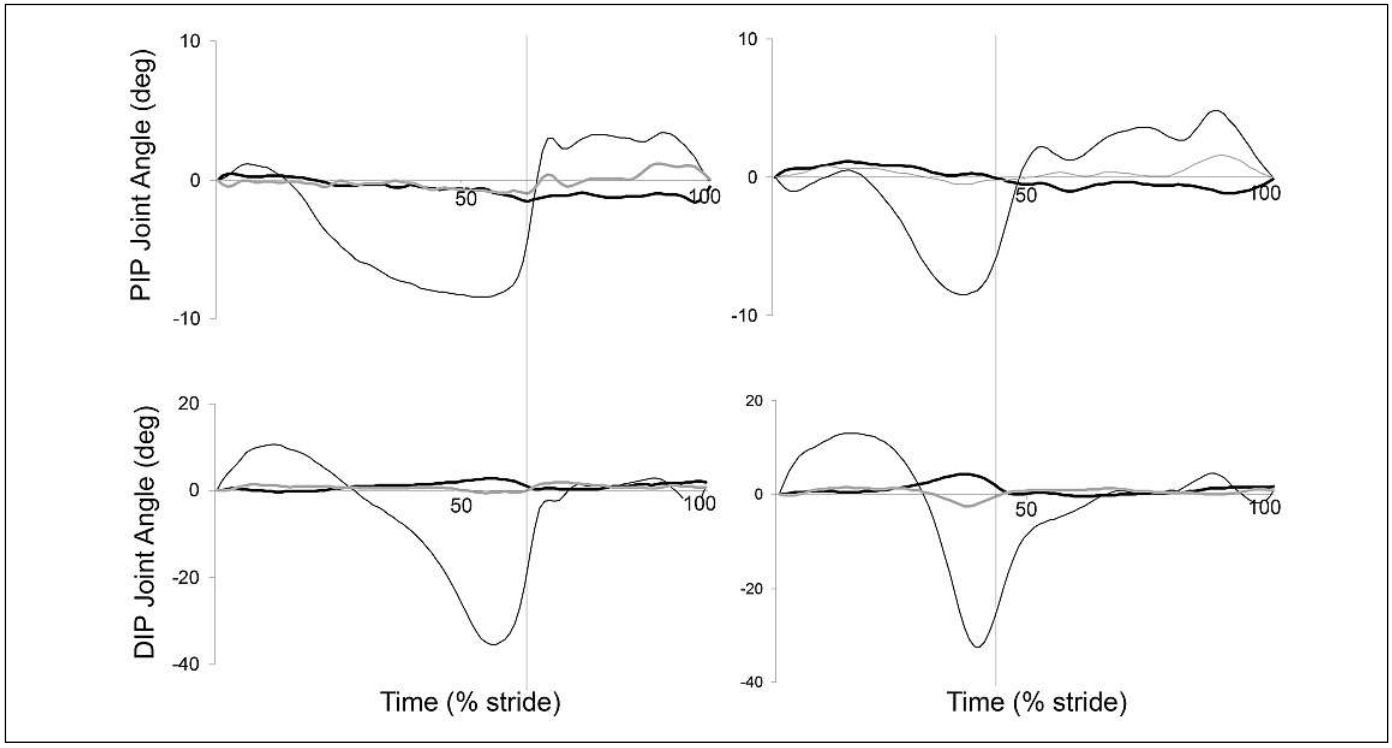

Fig. 2 Rotational kinematics of proximal interphalangeal (PIP) joint (above) and distal interphalangeal (DIP) joint (below) at walk (left column) and trot (right column). Values shown are flexion/extension (thin black line), internal/external rotation (thick black line) and adduction/abduction (grey line). Curves represent mean of four horses. Vertical lines indicate transition from stance to swing.

Proximal Interphalangeal Joint (PIP)

At the PIP joint, flexion/extension patterns for the two gaits (Fig. 2) were broadly similar when the relatively shorter stance duration of the trot was taken into account. The joint flexed during the impact phase, then extended through most of stance until just before lift off when the joint flexed rapidly in terminal stance and early swing. During the stance phase at walk, peak flexion (1.2 ± 0.7°) occurred at 6% of stride and peak extension (9.4 ± 1.7°) coincided with the start of breakover at 54% of stride. In trot, the PIP joint showed a little extension immediately after ground contact, then flexed, reaching a flexion peak (0.5 ± 2°) at 14% of stride, followed by peak extension (8.5 ± 0.6°) at 37% of stride, which also marked the start of breakover. In the swing phase, three flexion peaks could be distinguished at 69%, 78% and 91% of stride in walk and at 53%, 73% and 87% of stride in trot. These peaks were consistent in time of occurrence, though their magnitude varied between horses.

The internal/external rotation pattern at the PIP joint showed minimal variation between gaits and horses. There was a little internal rotation during impact that was then reversed so the joint became slightly externally rotated during swing. Adduction and abduction were minimal; there was a little abduction in late stance and a little adduction in late swing that coincided with the third flexion peak as the limb was prepared for ground contact with the lateral heel.

Distal Interphalangeal Joint (DIP)

At the DIP joint, the rotational patterns at walk and trot were consistent from stride to stride within each horse. Most of the movement patterns were also similar between horses (Fig. 2) with the exception of adduction/abduction in terminal stance. Immediately after ground contact, the DIP joint flexed rapidly with a little adduction and internal rotation in all horses. The joint then flexed more slowly to reach maximal flexion of 11 ± 2° at 13% of stride duration during walking, and 13 ± 4° at 16% of stride duration during trotting. In the second half of stance, the DIP joint extended by 36 ± 2° at walk and 34 ± 2° at trot relative to the angle at ground contact. During extension, the joint underwent a few degrees of internal rotation. Peak extension and internal rotation occurred around 57% stride at walk and at 40% stride at trot, which coincided with the middle of the breakover phase in both gaits (Fig. 2). In the second half of stance, two horses maintained a little abduction of the DIP joint relative to its angle at ground contact in both walk and trot, whereas the other two horses showed adduction in both gaits at this time (Fig. 2).

Swing phase rotations of the DIP joint were small, generally changing by less than 3° from the values at ground contact. In the sagittal plane, the flexion that began in late stance continued through early swing, returning the joint to its ground contact angle in early swing during walking and by midswing during trotting. In terminal swing, all horses showed some extension as the hoof was prepared for ground contact.

Discussion

In 3D analysis, each segment has its own coordinate system that is established in accordance with the anatomically meaningful axes of the bone. Joint angles are measured between the corresponding axes of the proximal and distal segments. By convention, joint movements are described in terms of the motion of the distal segment relative to a fixed proximal segment, but it should be remembered that the hoof is stationary on the ground during most of stance, so movements of the DIP joint at this time are actually due to motion of P2 relative to the stationary hoof.

The flexion/extension motion of the digital joints as defined by the BCS in this study may not be aligned with the sagittal plane of the horse's body, depending on the horse's conformation and the way the limb is placed on the ground. Even so, the shape of the DIP flexion/extension curves presented here are quite similar to 2D kinematic data reported in the GCS for the walk (9) and trot (3, 8). This was in spite of differences in the analytic planes between 2D and 3D kinematic analyses, and the fact that P1 and P2 were treated as a single rigid segment in the 2D studies. At the PIP joint, estimates of sagittal plane motion at trot based on the use of skin markers reported the correct pattern of motion but the amount of flexion in early stance was over-estimated as a consequence of skin displacement artifact (29-32).

The use of bone-fixed markers overcomes uncertainties associated with accurate identification and attachment of skin markers over bony landmarks on the short phalangeal bones, but skin markers must still be used to establish a bone-based coordinate system and to relate this coordinate system to the bone-fixed markers. Although the ranges of motion will not be affected, inaccuracies in skin marker placement during establishment of the BCS affect how much of the motion is ascribed to flexion versus extension, abduction versus adduction and internal versus external rotation. The study reported here relied on a combination of palpation and fluoroscopy to position skin markers for setting up the bone coordinate systems, whereas other researchers have used a template attached to the bones (5, 6). Since the digital joints have small dynamic ranges in the dorsal (adduction/abduction) and transverse (internal/external rotation) planes compared with the sagittal (extension/flexion) plane, motions measured in these planes are particularly sensitive to even slightly erroneous marker placement. Sagittal plane angles are also influenced by errors in marker placement, but the shape of the curve may appear 'normal' simply because the signal to noise ratio is better for the larger range measurements. In spite of differences in the methods for establishing the coordinate systems and the technologies used to track the markers, the results reported here show similar patterns and amplitudes of motion at the PIP and DIP joints during the stance phase at walk (5) and the stance phase when trotting on a treadmill (6). Unfortunately, swing phase data were not reported in these studies.

In vitro loading of cadaver limbs has suggested that flexion of the PIP joint increases exponentially with load (33). When the limb was loaded vertically to 6,000 N, which corresponds in magnitude to midstance loading at trot, the PIP joint showed 8.1° flexion (31). However, this type of loading does not accurately simulate the situation *in vivo*, in which peak flexion of the PIP joint occurs before midstance, when the vertical force is about 2,500 N at walk (9) and 3,000 N at trot (8). During *in vivo* recordings, the PIP joint is extending not flexing at midstance. The relatively small difference in vertical force at the time of peak PIP joint flexion in walk and trot may explain the similarity in peak flexion angles in the two gaits in the study reported here. PIP joint flexion *in vitro* varied greatly between horses, ranging from 3.1° to 14.5°, and it was suggested that this might have been related to differences in size between horses (31). However, the horses in our study also showed relatively large variability even though they were of similar sizes.

The flexion cycle in early stance at the PIP and DIP joints was followed by a larger cycle of extension that peaked during breakover. Extension is a consequence of the trunk moving forward over the grounded hoof, which extends the interphalangeal joints against a flexor torque (21, 32). When the flexor torque exceeds the extensor torque of the ground reaction force, which is diminishing at this time, breakover begins.

During breakover, horses vary as to whether they roll over the inside or outside of the hoof wall (33), which is likely to affect the direction of the DIP joint rotations during breakover. When trotting on a treadmill, seven of nine horses rolled over the outside of the toe and two rolled over to the inside (34). Interestingly, the two horses that rolled to the inside when barefoot, rolled to the outside when shod and two horses that had rolled to the outside when barefoot rolled to the inside when shod. The same authors found that the majority of horses showed a medial twisting of the hoof during breakover, which is equivalent to the internal rotation recorded here. Our results indicate that the DIP joint was abducted and internally rotated at the start of breakover, especially at trot, which is in accordance with the results of Chateau et al. (6).

During periods of high acceleration and deceleration at the beginning and end of the swing phase, inertial moments cause passive flexion and extension of the DIP and PIP joints due to the mass of the hoof in both walk (34) and trot (7, 35). As the hoof leaves the ground, the elbow flexors act concentrically to flex the elbow and protract the forearm, with the more distal joints flexing under the control of a net extensor moment due to tension in the common digital extensor tendon (36) and extensor branches (37), which control inertially driven movements of the inter-digital joints. In midswing, momentum carries the distal limb forward. Then, in the second half of swing, the elbow extensors work eccentrically to control protraction then concentrically to retract the forelimb prior to ground contact (32, 35). In early swing, the PIP and DIP joints return to their impact angles. Subsequently, swing phase flexion of the PIP joint relative to its impact angle is greater than that of the DIP joint as a consequence of the greater mass and, consequently, greater momentum of the digital segments distal to this joint. Swing phase flexion peaks occur concurrently at the PIP and DIP joints, though peaks in the DIP joint are smaller and less well defined. Similar peaks have been documented in the flexion/extension curves for the DIP joints in 2D data (3).

In the majority of cases, the first part of the hoof to contact the ground is the lateral heel (38, 39), though conformation, farriery or lameness may affect hoof orientation at contact and offer an explanation for inter-individual variations in the direction of joint motion during impact. One of the functions of the digital joints is to compensate for asymmetrical hoof placement due to uneven ground, turning sharply or hoof imbalance. Under these conditions, the weight-bearing limb rolls over the grounded hoof in both mediolateral and craniocaudal directions. Although the amounts of adduction/abduction and axial rotation are small during locomotion in a straight line on a level surface, *in vitro* loading with a 12° wedge on the medial or lateral side of the hoof has shown that involvement of the DIP and PIP joints in the compensation process varies with the amount of loading. Under low loading, the DIP joint compensates by showing more adduction/abduction and axial rotation, which increases the risk of over-use injuries to the supporting soft tissues that control motion outside of the sagittal plane (40). At higher loads there is greater involvement of the PIP and MCP joints in the compensation process (19). If this relationship is also true *in vivo*, it offers an explanation for the high incidence of osteoarthritis of the PIP joint (high ringbone) in horses competing in sports that combine speed with abrupt changes of direction (41). Kinetic analyses will provide further information on the joint functions and the causes and effects of specific lamenesses.

For horses moving at walk and trot on a flat surface, the most important loss of motion following PIP arthrodesis is extension in late stance, which is likely to be compensated primarily by the DIP joint. The fact that 46% (42) to 67% (43) of horses returned to athletic soundness after PIP arthrodesis indicates that other joints are able to compensate adequately for the loss of motion. However, the increase in DIP joint extension may explain the exacerbation of DIP joint pain that has been observed following PIP arthrodesis (43). For horses working on uneven ground or turning abruptly, the DIP and MCP joints must compensate for loss of axial rotation and adduction/abduction in the arthrodesed PIP joint, which may increase the risk of injury, especially to the collateral ligaments of the DIP. Thus, mediolateral hoof balance is particularly important in horses with PIP arthrodesis. During the swing phase, loss of approximately 5° of flexion following PIP joint arthrodesis is unlikely to cause problems, assuming the more proximal joints are able to raise the hoof clear of the ground.

Due to the invasive nature of the procedure used to fix the markers to the bones, the number of subjects was kept to a minimum, which did not give sufficient statistical power to make comparisons between the two gaits. However, the ranges of motion and the amounts of flexion and extension appeared quite similar for the limited range of speeds evaluated here at walk and trot. This is in contrast to the MCP joint in which peak extension during stance is speed dependent (44). The flexion/extension curves of the PIP or DIP joints do not appear to be strongly influenced by the vertical force which peaks in midstance, and the timing of the joint movements suggests that they may be more sensitive to the longitudinal force.

In summary, this study presents 3D rotations of the digital joints at walk and trot. The results indicate that flexion/extension is the dominant rotation at the PIP and DIP joints. The patterns and amplitudes of movement at the digital joints are very similar during walking and trotting and, within the range of speeds evaluated, did not appear to show gait or speed dependent changes in amplitude. The range of motion for flexion/extension at the PIP joint (13° at walk and 14° at trot) is sufficiently large to raise the question as to whether this joint should be regarded as a low motion joint. Arthrodesis techniques should take account of the need for the DIP joint to compensate for loss of PIP joint extension in late stance. The DIP joint shows larger ranges of motion in all three directions than the PIP joint during locomotion in a straight line on a level surface, but the possibility of rotational motion outside of the sagittal plane is thought to be important for allowing the digit to accommodate to different hoof angulations relative to the ground during lateral or turning movements and to compensate for mediolateral imbalances of the bearing surface.

References

1. Schryver HF, Bartel DL, Langrana N et al. Locomotion in the horse: kinematics and external and internal forces in the normal equine digit in walk and trot. Am J Vet Res 1978; 39: 1728–1733.
2. Riemersma DJ, Schamhardt HC, Hartman W et al. Kinetics and kinematics of the equine hind limb: In vivo tendon loads and force plate measurements in ponies. Am J Vet Res 1988; 49: 1344–1352.
3. Back W, Schamhardt HC, Savelberg HHCM et al. How the horse moves: significance of graphical representations of equine forelimb kinematics. Equine Vet J 1995; 27: 31–38.
4. Clayton HM, Sha DH, Stick JA et al. Three-dimensional carpal kinematics of trotting horses. Equine Vet J, 2004; 36: 665–670.
5. Chateau H, Degueurce C, Denoix J-M. Evaluation of three-dimensional kinematics of the distal portion of the forelimb in horses walking in a straight line. Am J Vet Res 2004; 65: 447–455.
6. Chateau H, Deguerce C, Denoix J-M. Three-dimensional kinematics of the distal forelimb in horses trotting on a treadmill and effects o elevation of heel and toe. Equine Vet J 2006; 38: 164–169.
7. Lanovaz JL, Clayton HM, Colborne GR et al. Forelimb kinematics and net joint moments during the swing phase of the trot. Equine Vet J 1999; Supplement 30: 235–239.
8. Clayton HM, Willemen MA, Schamhardt HC et al. Kinematics and ground reaction forces in horses with superficial digital flexor tendinitis. Am J Vet Res 2000; 61: 191–196.
9. Hodson E, Clayton HM, Lanovaz JL The forelimb of walking horses: 1. Kinematics and ground reaction forces. Equine Vet J 2000; 32: 287–294.
10. Reinschmidt C, van den Bogert AJ, Murphy N et al. Tibiocalcaneal motion during running measured with external and bone markers. Clin Biomech 1997; 12: 8–16.
11. Weeren PR van, Bogert AJ van den, Barneveld A. Correction models for skin displacement in equine kinematic gait analysis. J Equine Vet Sci 1992; 12: 178–192.
12. Lanovaz JL, Khumsap S, Clayton HM. Quantification of three-dimensional skin displacement artefacts on the equine tibia and third metatarsus. Equine Compar Exerc Physiol 2004; 1: 141–150.
13. Sha DH, Mullineaux DR, Clayton HM. A three-dimensional analysis of patterns of skin displacement over the equine radius. Equine Vet J 2004; 36: 671–676.
14. Lafortune MA, Cavanagh PR, Sommer HJ et al. Three-dimentional kinematics of the human knee during walking. J Biomech 1992; 25: 347–357.
15. Lanovaz JL, Khumsap S, Clayton HM et al. Three-dimensional kinematics of the tarsal joint at the trot. Equine Vet J 2002; Suppl. 34: S308–313.
16. Chateau H, Degueurce C, Denoix J-M. Effects of 6° elevation of the heels on 3D kinematics of the distal portion of the forelimb in the walking horse. Equine Vet J 2004; 36: 649–654.
17. Chateau H, Deguerce C, Jerbi H et al. Three-dimensional kinematics of the equine interphal-

angeal joint: articular impact of asymmetric bearing. Vet Res 2002; 33: 371–382.
18. Dyson S, Murray R, Schramme M et al. Lameness in 46 horses associated with deep digital flexor tendonitis confirmed with magnetic resonance imaging. Equine Vet J 2003; 35: 681–690.
19. Clayton HM, Lanovaz JL, Schamhardt HC et al. Net joint moments and powers in the equine forelimb in the stance phase of the trot. Equine Vet J 1998; 30: 384–389.
20. Colborne GR, Lanovaz JL, Sprigings EJ et al. Forelimb joint moments and power during the walking stance phase of horse. Am J Vet Res 1998; 59: 609–614.
21. Clayton HM, Schamhardt HC, Lanovaz JL et al. Net joint moments and joint powers in horses with superficial digital flexor tendinitis. Am J Vet Res 2000; 61: 197–201.
22. Cappozzo A, Croce UD, Leardini A et al. Human movement analysis using sterophotogrammetry, Part 1: theoretical background. Gait and Posture 2005; 21: 186–196.
23. Grood EW, Suntay WJ. A joint coordinate system for the clinical description of three-dimensional motions: applications to the knee. J Biomech Eng 1983; 105: 136–144.
24. Soderkvist I, Wedin PA. Determining the movements of the skeleton using well-configured markers. J Biomech 1993; 26: 1473–1477.
25. Spoor CW, Veldpaus FE. Rigid body motion calculated from spatial co-ordinates of markers. J Biomech 1980; 13: 391–393.
26. Woltring HJ. 3-D attitude representation of human joints: a standardization proposal. J Biomech 1994; 27: 1399–1414.
27. Drevemo S, Johnston C, Roepstorff L et al. Nerve block and intra-articular anesthesia of the forelimb in the sound horse. Equine vet J 1999; Suppl. 30: S266–269.
28. Johnston C, Gottlieb-Vedi M, Drevemo S et al. The kinematics of loading and fatigue in the Standardbred trotter. Equine Vet J 1999; Suppl. 30: S249–53.
29. Roepstorff L, Johnston C, Drevemo S. The effect of shoeing on kinetics and kinematics during the stance phase. Equine Vet J 1999; Suppl. 30: S279–285.
30. Clayton HM, Singleton WH, Lanovaz JL et al. Sagittal plane kinematics and kinetics of the pastern joint during the stance phase of the trot. Vet Comp Orthop Traumatol 2002; 15: 15–17.
31. Degueurce C, Chateau H, Jerbi H et al. Three-dimensional kinematics of the proximal interphalangeal joint: effects of raising the heels or the toe. Equine Vet J 2001; Suppl. 33: 79–83.
32. Clayton HM, Hodson EF, Lanovaz JL. The forelimb in walking horses: 2. Net joint moments and joint powers. Equine Vet J 2000; 32: 295–299.
33. Williams G, Deacon M. Hoof capsule deviations. In: No foot, no horse. Kenilworth Press, Addington, UK. 1991; 71.
34. Caudron I, Grulke S, Farnir F et al. In-shoe force sensor to assess hoof balance determined by radiographic method in ponies trotting on a treadmill. Vet Quart 1998; 20: 131–135.
35. Singleton WH, Clayton HM, Lanovaz JL et al. Effects of shoeing on forelimb swing phase kinetics of trotting horses. Vet Comp Orthop Traumatol 2003; 16: 16–20.
36. Barnes GRG, Pinder DN. *In vivo* tendon tension and bone strain measurement and correlation. J Biomech 1974; 7: 35–42.
37. Jansen MO, van Buiten A, van den Bogert AJ et al. Strain of the musculus interosseus medius and its rami extensorii in the horse, deduced from in vivo kinematics. Acta Anat 1993; 147: 118–124.
38. Wilson AM, Seelig TJ, Shield RA et al. The effect of hoof imbalance on point of force application in the horse. Equine Vet J 1998; 30: 540–545.
39. Van Heel MCV, Barneveld A, van Weeren PR et al. Dynamic pressure measurements for the detailed study of hoof balance: the effect of trimming. Equine Vet J 2004; 36: 778–782.
40. Keegan KG, Satterley JM, Skubik M et al. Use of gyroscopic sensors for objective evaluation of trimming and shoeing to alter time between heel and toe lift-off at end of the stance phase in horses walking and trotting on a treadmill. Am J Vet Res 2005; 66: 2046–2054.
41. Ruggles AJ. The proximal and middle phalanges and proximal interphalangeal joint. In: Diagnosis and management of lameness in the horse. Ross MW, Dyson SJ (eds). Philadelphia: W.B. Saunders 2003; 342–348.
42. Caron JP, Fretz PB, Bailey JV et al. Proximal interphalangeal arthrodesis in the horse: a retrospective study and modified screw technique. Vet Surg 1990; 19: 196.
43. Martin GS, McIlwraith CW, Turner AS et al. Long-term results and complications of proximal interphalangeal arthrodesis in horses. J Am Vet Med Assoc 1984; 184: 1136–1140.
44. McGuigan PM, Wilson AM. The effect of gait and digital flexor muscle activation on limb compliance in the forelimb of the horse *Equus caballus*. J Exp Biol 2003; 206: 1325–1336.

Correspondence to:
Hilary Clayton
Michigan State University
Large Animal Clinical Sciences
D202 Veterinary Medical Center
East Lansing, Michigan 48824–1314
USA
Phone: +1 517 432 5630, Fax: +1 517 432 3442
E-mail: claytonh@cvm.msu.edu